

Histone deacetylase inhibition decreases proliferation and potentiates the effect of ionizing radiation in atypical teratoid/rhabdoid tumor cells

Jeffrey A. Knipstein, Diane K. Birks, Andrew M. Donson, Irina Alimova, Nicholas K. Foreman, and Rajeev Vibhakhar

Department of Pediatrics, Section of Pediatric Hematology/Oncology/BMT, University of Colorado Denver (J.A.K., D.K.B., A.M.D., I.A., N.K.F., R.V.) and Section of Pediatric Hematology/Oncology/BMT, Children's Hospital Colorado, Aurora, Colorado (J.A.K., N.K.F., R.V.)

Atypical teratoid/rhabdoid tumor (ATRT) is a highly malignant central nervous system neoplasm that primarily occurs in children less than 3 years of age. Because of poor outcomes with intense and toxic multimodality treatment, new therapies are urgently needed. Histone deacetylase inhibitors (HDIs) have been evaluated as novel agents for multiple malignancies and have been shown to function as radiosensitizers. They act as epigenetic modifiers and lead to re-expression of inappropriately repressed genes, proteins, and cellular functions. Because of the underlying chromatin remodeling gene mutation in ATRT, HDIs are ideal candidates for therapeutic evaluation. To evaluate the role of HDIs against ATRT in vitro, we assessed the effect of drug treatment on proliferation, apoptosis, and gene expression. In addition, we examined HDI pretreatment as a radiosensitization strategy for ATRT. 3-(4,5-dimethylthiazol-2-yl)-5-(3-carboxymethoxyphenyl)-2-(4-sulfophenyl)-2H-tetrazolium with phenazine methosulfate electron coupling reagent (MTS) and clonogenic assays demonstrated that HDI treatment significantly reduces the proliferative capacity of BT-12 and BT-16 ATRT cells. In addition, the HDI SNDX-275 was able to induce apoptosis in both cell lines and induced p21^{Waf1/Cip1} protein expression as measured by Western blot. Evaluation of differential gene expression by microarray and pathway analysis after HDI treatment demonstrated alterations of several key ATRT cellular functions. Finally, we showed that HDI pretreatment effectively potentiates the effect of

ionizing radiation on ATRT cells as measured by clonogenic assay. Our findings suggest that the addition of HDIs to ATRT therapy may prove to be beneficial, especially when administered in combination with current treatment modalities, such as radiation.

Keywords: ATRT, HDAC inhibitor, radiosensitization.

A typical teratoid/rhabdoid tumor (ATRT) is a malignant central nervous system (CNS) tumor that was initially distinguished from other pediatric embryonal brain tumors in the mid-1980s.^{1,2} It most commonly affects young children and historically carries a poor outcome.^{3–5} Therapy for this tumor is frequently multimodality in nature, involving surgery, radiation, and chemotherapy.⁵ In the past 10 years, therapy has either focused on high-dose chemotherapy with autologous stem cell rescue or, more recently, use of a regimen based on sarcoma therapy.^{6,7} Despite an increase in overall survival with these approaches, therapy related toxicity frequently remains a critical problem in this young age group. ATRT is frequently associated with a mutation or deletion of the *hSNF5/INI1/SMARCB1* gene found on chromosome 22q.^{8,9} *SMARCB1* functions as a tumor suppressor, and its absence has been shown to be associated with increased markers of cell cycle progression.¹⁰ Because *SMARCB1* is a member of the SWI/SNF chromatin remodeling complex, therapeutic agents, such as histone deacetylase inhibitors (HDIs), that affect chromatin structure may prove to be effective in ATRT.

In recent years, the mechanisms of HDIs have been evaluated in multiple models of malignancies and, because of in vitro and in vivo efficacy, have begun to emerge as promising therapies.^{11–16} Thus far, suberoylanilide hydroxamic acid (SAHA; vorinostat) and

Received February 22, 2011; accepted October 24, 2011.

Corresponding Author: Jeffrey Knipstein, MD, Children's Hospital Colorado, 13123 E 16th Ave, B-115, Aurora, CO 80045 (jeffrey.knipstein@childrenscolorado.org).

romidepsin (depsipeptide) have been Food and Drug Administration approved for the treatment of cutaneous T-cell lymphoma; however, multiple HDIs are currently in development.^{17,18}

HDIs function by increasing acetylation of histones at lysine residues, thus blocking the physiologic role of histone deacetylase (HDAC). Increased acetylation is also seen with nonhistone proteins.¹⁹ Histone acetylation permits a more open chromatin configuration, thus allowing more access for transcription factors and transcriptional molecules. Several antiproliferative cellular functions are often among those derepressed; this includes processes such as growth arrest, apoptosis, and cell cycle inhibition. In addition, HDI treatment is associated with decreased metastatic potential and angiogenesis.¹⁶

Because of the role of HDIs as promoters of cell cycle inhibition,¹⁶ ATRT is a particularly interesting model for evaluation of these agents because of its association with increased cyclin D1 expression.¹⁰ In addition, because ATRT is a tumor that frequently requires radiation as part of its therapy, HDIs are of particular interest, as previous literature has discussed their role in radiosensitization of other types of malignancies.^{20–23}

Previous studies^{24–27} have analyzed some aspects of rhabdoid tumor treatment with HDIs, but to date, none have examined the capacity of HDIs to alter the effect of radiation in ATRT. In this study, we evaluated the HDI-induced alteration of in vitro proliferative capacity of ATRT cell lines and a primary patient sample. In addition, we examined the effect of HDI treatment on apoptosis, tumor suppressor protein expression, and differential gene expression. Finally, the ability of HDI treatment to potentiate the effect of radiation on ATRT cell lines was studied.

Materials and Methods

Cell Culture and HDAC Inhibitors

BT-12 and BT-16 ATRT cells were kindly provided as a gift from Dr. Peter Houghton's laboratory (St. Jude Children's Research Hospital). Cells were cultured in RPMI-1640 (Invitrogen) supplemented with 10% fetal bovine serum according to the supplier's recommendations. Primary, short-term cell culture (UPN737) was derived from an immediate postsurgical specimen under a protocol approved by the institutional review board at the University of Colorado. Primary cell culture was generated as previously described.²⁸ Cultures were maintained at low passage number (p2–p4) in RPMI-1640 supplemented with 20% fetal bovine serum. Cell lines were propagated at 37°C in 5% CO₂ with humidity.

The HDIs trichostatin A (TsA), SAHA, and SNDX-275 (Sigma) were diluted in DMSO to appropriate concentrations.

Cell Viability Assay

The effect of HDIs on BT-12, BT-16, and UPN737 cells was analyzed with Cell Titer Aqueous (Promega)

3-(4,5-dimethylthiazol-2-yl)-5-(3-carboxymethoxyphenyl)-2-(4-sulfophenyl)-2H-tetrazolium with phenazine methosulfate electron coupling reagent (MTS) assay as previously described.²⁹ In brief, cells were plated in triplicate in 96-well plates for 24 h. Subsequently, TsA, SAHA, or SNDX-275 was added in 2-fold serial dilutions at 4 nM–1 μ M (TsA) and 125 nM–128 μ M (SAHA and SNDX-275). DMSO was added to control wells. After 72 h, 20 μ L of MTS reagent was added to each well and the absorbance measured at 490 nm using a microplate reader (BioTek). Relative cell number was calculated by normalizing the absorbance of HDI-treated samples to controls; 50% inhibitory concentrations (IC₅₀) and 25% IC (IC₂₅) were calculated using GraphPad Prism software.

Clonogenic Assay

BT-12 and BT-16 cells were seeded on a 10 cm² culture plate (300 000 cells/plate) for 24 h. SNDX-275 was then added to separate plates at concentrations equivalent to IC₅₀ (per MTS assay analysis), IC₂₅, and 2-fold serial dilutions downward from IC₂₅. Controls were treated with DMSO. SNDX-275 or DMSO was removed after 48 h, and the cells were collected. Viable cells were counted by trypan blue exclusion. Cells were then seeded in triplicate per treatment condition into 6-well plates (400 cells/well) for clonogenic assay and allowed to grow in culture medium. After sufficient colony formation was demonstrated in control wells, cells were washed with phosphate-buffered saline (PBS) and then stained with crystal violet. Colonies were defined as those with more than 50 cells and were then counted. Analysis was performed with GraphPad Prism software.

Protein Collection and Western Blotting

Western blotting was performed per standard methods. In brief, BT-12 and BT-16 cells were treated with 1 μ M SNDX-275 for 0, 3, 6, 24, and 48 h. Drug was then removed, and 2 further time points at 6 and 24 h after removal were obtained. At each time point, cells were collected, washed with PBS, resuspended in chilled RIPA buffer and Protease Inhibitor Cocktail (Roche), incubated on ice for 15 min, and centrifuged for 30 min. Protein quantification was performed using the Bradford assay. Incubation of protein lysates with Laemmli sample buffer (Bio-Rad) was performed at 95°C for 5 min. Samples were then subjected to SDS-PAGE (15% Tris-HCl precast gel; Bio-Rad) and transferred onto a polyvinylidene fluoride (PVDF) membrane. Immunoblotting was performed using the Snap I.D. system (Millipore) with primary [p21^{Waf1/Cip1} (BD Biosciences), actin (Chemicon)] and HRP-conjugated secondary (Jackson Laboratories) antibodies. Chemiluminescence was elicited with SuperSignal West pico and femto substrates (Pierce Scientific) and then exposed to film.

Apoptosis Assay

Both ATRT cell lines were seeded in triplicate into 6-well plates for 24 h. Cells were treated with IC₅₀ of SNDX-275 (per MTS assay analysis) versus DMSO control for 24, 48, or 72 h. At the specified time points, media (inclusive of de-adherent cells) and adherent cells were collected, centrifuged, and counted by ViaCount assay on a Guava EasyCyte flow cytometer (Millipore). For each time point, 30 000 cells per cell line were incubated with Nexin reagent (Annexin V-PE and 7-AAD, Millipore) for 20 min. Cell fluorescence was measured and analyzed on the Guava EasyCyte flow cytometer. Numerical differences in apoptotic fractions were analyzed using GraphPad Prism software.

Gene Array and Pathway Analysis

BT-12 and BT-16 cells were treated with IC₂₅ (as measured by MTS assay) of SNDX-275 or DMSO (control) for 24 h. Total RNA was collected using the RNeasy kit (Qiagen). RNA was hybridized to HG-U133 Plus 2.0 GeneChips (Affymetrix). Results of the gene array were normalized with Gene-Chip robust multiarray average (gcRMA) software, resulting in log₂ expression values. Genes with either an increase or decrease by 1.75-fold change (0.8 log₂) between treated and control in both cell lines were selected for further evaluation by Ingenuity Pathway Analysis (IPA; Ingenuity Systems). Gene lists with mean fold changes were subjected to IPA, and differentially altered networks and biologic function lists were generated with corresponding scores or *P* value ranges, respectively. The data discussed in this publication have been deposited in NCBI's Gene Expression Omnibus (GEO)³⁰ and are accessible through GEO Series accession number GSE31122 (<http://www.ncbi.nlm.nih.gov/geo/query/acc.cgi?acc=GSE31122>).

Real-Time Quantitative Reverse-Transcriptase Polymerase Chain Reaction

cDNA was generated according to the manufacturer's instructions using reverse transcription with mRNA isolated in the gene array experiment and the Mastercycler personal thermal cycler (Eppendorf). Real-time quantitative polymerase chain reaction (PCR) was performed using the StepOne Plus detection system (Applied Biosystems). Taqman reagents (Applied Biosystems) were used according to the manufacturer's recommendations. Gene expression was determined by the ΔCt method. All assays were performed in triplicate.

HDI Radiosensitization Colony Formation Assay

BT-12 and BT-16 cells were seeded into 6-well plates and subsequently treated with SNDX-275 at 1 and 2 μM concentrations and DMSO (control) for 24 h. Cells were then collected, and live cells were quantified using trypan blue exclusion. For each concentration,

500 cells were seeded per well in triplicate on 6-well plates. Four hours after drug removal, cells were subjected to X-irradiation at doses of 0, 0.5, 1, 2, 2.5, 3, 4, or 5 Gy. Colony formation proceeded until sufficient colony growth was demonstrated in control wells. Media was then removed; cells were washed with PBS and then were stained with crystal violet. Colonies were defined as more than 50 cells and were then counted. Statistical analysis was performed using GraphPad Prism software.

Statistical Analysis

Data obtained from these experiments were processed using Excel (Microsoft), Prism (GraphPad), and gcRMA software, for gene array normalization. IC₅₀ and IC₂₅ were determined using nonlinear regression. Sensitizer enhancement ratios were calculated by dividing the radiation dose of DMSO-treated controls at a specified survival fraction by the radiation dose of the SNDX-275-treated cells at the same survival fraction. Radiation doses at the specified survival fractions were calculated using nonlinear regression analysis of survival curves. All experiments, with the exception of the microarray analysis, were performed, at minimum, independently in triplicate to allow for appropriate statistical analysis. Error bars, unless otherwise indicated, represent the standard error of the mean.

Results

HDIs Decrease In Vitro Proliferation of ATRT Cell Lines

To measure the effect of HDAC inhibition on cell proliferation, BT-12, BT-16, and UPN737 ATRT cells were treated with TsA, SAHA, and SNDX-275. Addition of TsA, SAHA, and SNDX-275 to BT-12 and BT-16 cells and SNDX-275 to the primary patient sample UPN737 resulted in a decrease of metabolically active cells 72 h after drug treatment, as measured by MTS assay (Fig. 1A–C). Incubation with TsA resulted in the lowest IC₅₀ (BT-12: 253 nM; BT-16: 207 nM). IC₅₀ for SAHA (BT-12: 3.8 μM ; BT-16: 0.82 μM) and SNDX-275 (BT-12: 2.21 μM ; BT-16: 1.61 μM ; UPN737: 2.49 μM) treatments were higher but remained in the low micromolar range. Of note, the patient sample UPN737 exhibited an IC₅₀ for SNDX-275 that was comparable to that of the BT-12 and BT-16 cell lines (Fig. 1D).

As a measure of long-term cellular proliferation, BT-12 and BT-16 cell lines were treated with SNDX-275 for 48 h and then evaluated by clonogenic assay. SNDX-275 treatment was associated with decreased colony formation in a dose-dependent manner for both cell lines (Fig. 2, Supplementary Fig. S1). Statistically significant differences (*P* < .05) were achieved at the 54 nM concentration for BT-16 and 704 nM concentration for BT-12, consistent with

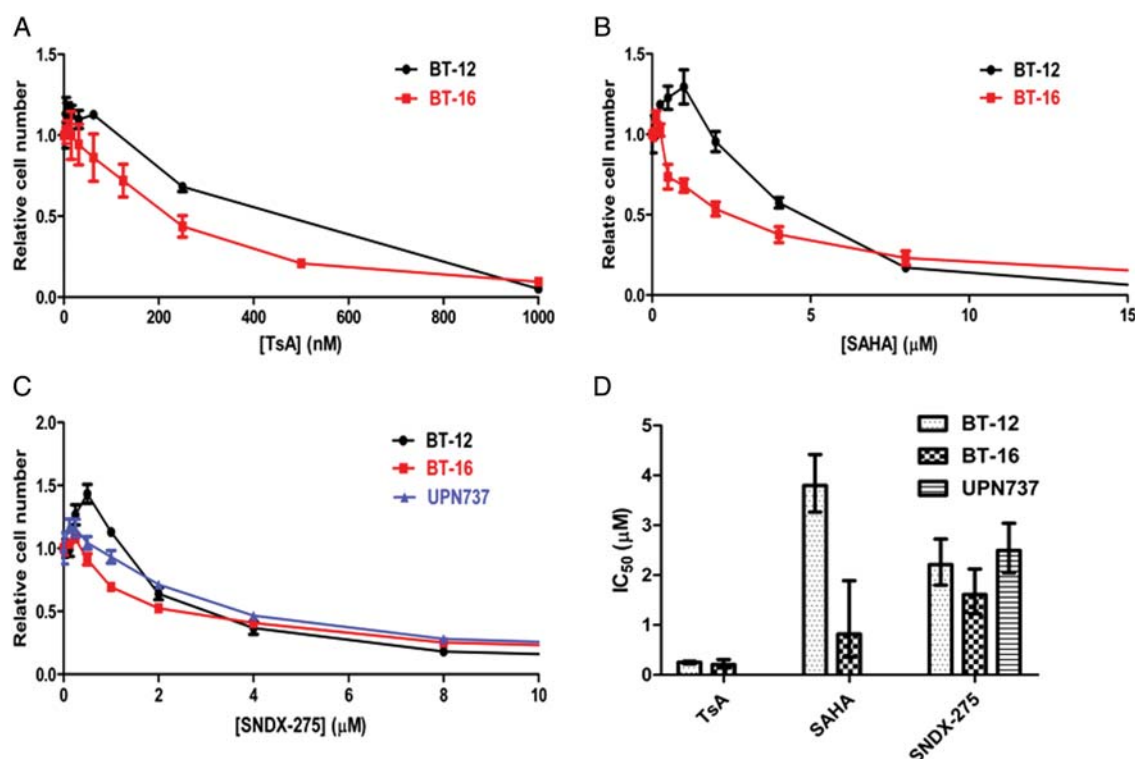


Fig. 1. Histone deacetylase inhibitor (HDI) treatment decreases atypical teratoid/rhabdoid tumor (ATRT) cell proliferation, as measured by MTS assay. Graphs of relative BT-12, BT-16, and UPN737 (Fig. 1C only) cell numbers versus HDI concentration: (A) Trichostatin A (TsA), (B) Suberoylanilide hydroxamic acid (SAHA), and (C) SNDX-275. Concentrations tested for SAHA and SNDX-275 extended to 128 μM (not shown). (D) Summary of IC₅₀ values obtained for the 3 HDIs tested.

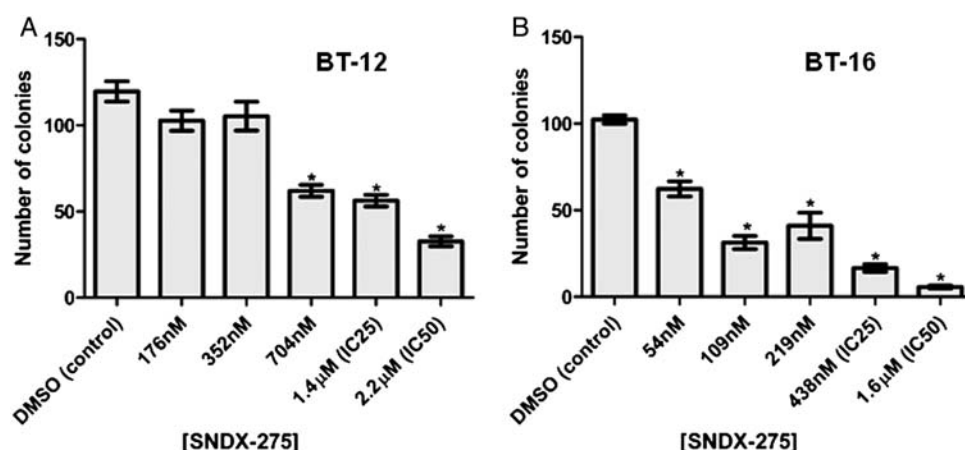


Fig. 2. SNDX-275 decreases atypical teratoid/rhabdoid tumor (ATRT) cell colony formation in clonogenic assay. BT-12 (A) and BT-16 (B) colony numbers after treatment with serial dilutions of SNDX-275. * $P < .05$ relative to DMSO-treated control.

previous results from MTS assays demonstrating a higher IC₅₀ for BT-12 cells.

SNDX-275 Promotes Increased p21^{Waf1/Cip1} Expression

The tumor suppressor protein p21^{Waf1/Cip1} is frequently implicated in growth arrest and is known to be induced by HDI treatment.¹⁶ To determine whether treatment

with SNDX-275 increases p21^{Waf1/Cip1} expression in ATRT, Western blotting of protein samples from BT-12 and BT-16 cell lines was performed. Cells were treated with 1 μM SNDX-275 for 0, 3, 6, 24, or 48 h. Treatment with SNDX-275 resulted in increased p21^{Waf1/Cip1} expression, with maximum expression demonstrated after 24 h of drug exposure (Fig. 3). After SNDX-275 was removed from the culture medium, p21^{Waf1/Cip1} expression decreased but continued at 6 and 24 h after removal.

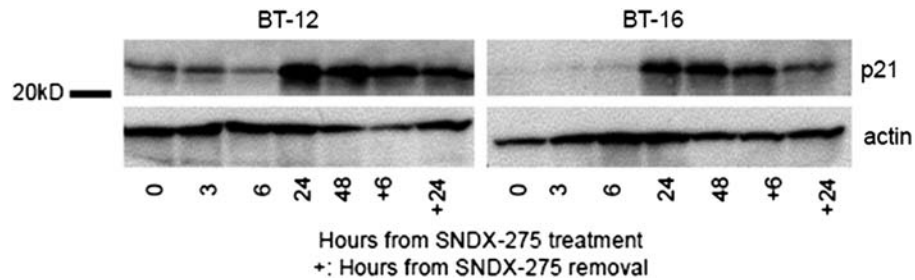


Fig. 3. SNDX-275 increases p21 expression in atypical teratoid/rhabdoid tumor (ATRT) cells. Western blot from cell lysates obtained after SNDX-275 treatment. Maximal p21 expression can be seen at 24 h post-treatment.

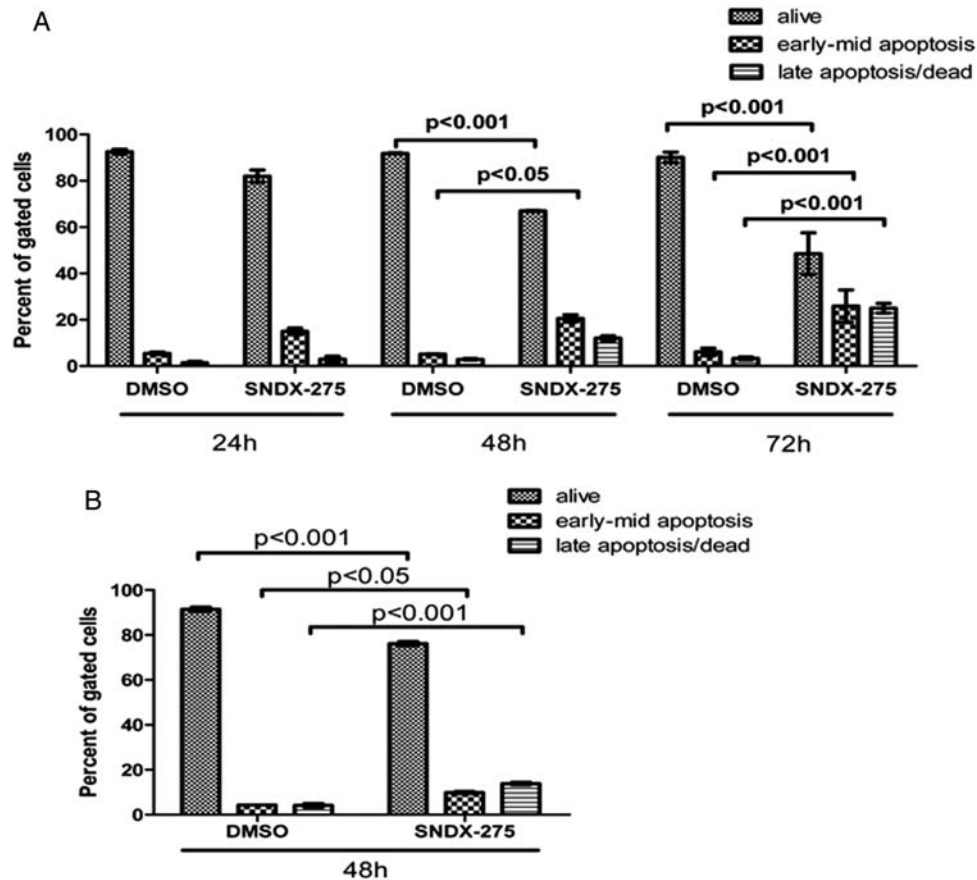


Fig. 4. SNDX-275 induces apoptosis in atypical teratoid/rhabdoid tumor (ATRT) cells. Nexin assay for apoptosis in BT-12 (A) and BT-16 (B) cells with DMSO or SNDX-275. Early apoptosis and subsequently late apoptosis/death increases with SNDX-275 incubation.

SNDX-275 Induces Apoptosis in BT-12 and BT-16 Cell Lines

To evaluate the effect of SNDX-275 treatment on apoptosis, BT-12 and BT-16 cells were treated for 24, 48, and 72 h with concentrations of SNDX-275 corresponding to IC_{50} obtained from the MTS assay analysis. Control samples were treated with DMSO. Apoptosis was measured by Nexin assay (7-AAD and Annexin V-PE). In BT-12 cells, a nonstatistically significant apoptotic effect was seen starting at 24 h after SNDX-275 treatment (Fig. 4A, Supplementary Fig. S2). Early-mid apoptotic and late apoptotic/dead fractions represented

5.5% versus 14.9% (mean values, DMSO vs. SNDX-275) of gated cells and 1.4% versus 2.9%, respectively. At 48 h, statistically significant differences in alive and early-mid apoptotic cell fractions were demonstrated (alive: 91.8% vs. 67%, $P < .001$; early-mid apoptotic: 5.1% vs. 20.6%, $P < .05$). After 72 h of drug exposure, all fractions of gated cells were statistically significant (alive: 90.1% vs. 48.5%, $P < .001$; early-mid apoptotic: 6.1% vs. 25.9%, $P < .001$; late apoptotic/dead: 3.3% vs. 24.9%, $P < .001$).

SNDX-275 also induced apoptosis in BT-16 cells; however, the effect did not become evident until 48 h after drug treatment (Fig. 4B, Supplementary Fig. S2).

Table 1. SNDX-275 exposure affects several key pathways in atypical teratoid/rhabdoid tumor (ATRT) cells.

Network	Molecules involved	Score
Nervous system development and function	27	44
Cellular growth and proliferation	27	44
Cell morphology	23	35
Cardiovascular/Metabolic disease	21	30
Cellular function and maintenance	20	28
Organismal development	20	27
Neurological disease	21	27
Cell-to-cell signaling and interaction	19	25
DNA replication, recombination, and repair	18	24
Cell cycle	17	22

Note: Top 10 biologic networks in BT-12 and BT-16 ATRT cells altered by 24 h exposure to IC₂₅ concentrations of SNDX-275 as assessed by Ingenuity Pathway Analysis of mRNA microarray data. Score = $-\log(\text{Fischer's exact test result})$.

At 48 h, statistically significant differences were seen in all fractions of gated BT-16 cells (DMSO vs. SNDX-275, alive: 91.5% vs. 76.1%, $P < .001$; early-mid apoptotic: 4.3% vs. 9.8%, $P < .05$; late apoptotic/dead: 4.1% vs. 13.8%, $P < .001$).

Treatment with SNDX-275 Leads to Alterations of Several Key Biological Networks and Functions

Because HDIs are known to alter several cellular functions, gene array analysis was performed on BT-12 and BT-16 ATRT cells after SNDX-275 treatment to identify key pathways affected by drug treatment. Total mRNA was collected after 24 h of SNDX-275 exposure, and gene array analysis was performed. After normalization using gcRMA software, the analysis produced a group of 396 differentially upregulated and 71 differentially downregulated genes shared by both cell lines (1.75 minimum fold-change from DMSO-treated controls). Gene lists were then analyzed using IPA. The top 10 differentially altered biologic networks are listed in Table 1, and the top 30 differentially altered biologic functions are listed in Supplementary Table S1. In IPA, networks are defined as collections of interconnected molecules assembled by a network algorithm. Of note, for this study, networks such as cellular growth and proliferation; DNA replication, recombination, and repair; and cell cycle were 3 of the networks identified as being altered by SNDX-275 treatment.

To validate gene expression from the microarray data, real-time quantitative PCR was performed from mRNA isolated during the gene array experiment. Two of the genes significantly upregulated by SNDX-275 treatment in both cell lines were *CDKN2B* (p15) and *CDKN2D* (p19), both of which function as inhibitors of cyclin-dependent kinase 4 (CDK4) and inhibit cell cycle progression. In concordance with the microarray data, both of these genes were found to be statistically significantly upregulated by real-time quantitative PCR analysis (Supplementary Fig. S3).

SNDX-275 Potentiates the Effect of Radiation on ATRT Cell Colony Formation

To test the hypothesis that HDAC inhibition in ATRT cells would potentiate the effect of radiation, BT-12 and BT-16 cells were treated with DMSO or SNDX-275 (1 or 2 μM) for 24 h prior to receiving varying doses of X-irradiation. Samples were then analyzed for cellular proliferation by colony formation assay. For both BT-12 and BT-16 cell lines, SNDX-275 pretreatment was found to decrease colony formation after irradiation, compared with the individual doses of radiation alone. Figure 5A and B illustrates colony formation versus radiation as a function of SNDX-275 dose. As shown in Fig. 5C, colony formation was statistically significantly decreased at the lowest radiation dose (0.5 Gy). As a standard measure of radiosensitization, sensitizer enhancement ratios (SERs) were then calculated at survival fractions of 10% (SF_{0.1}) and 50% (SF_{0.5}). SF_{0.1} and SF_{0.5} radiation doses were determined using nonlinear regression analysis of survival curves (Supplementary Fig. S4). For BT-12, SERs at SF_{0.1} were 1.57 and 1.55 for the 1 μM and 2 μM SNDX-275 doses, respectively, and SERs at SF_{0.5} were 1.68 (1 μM SNDX-275) and 1.69 (2 μM SNDX-275). The BT-16 cell line demonstrated increased sensitivity to the combination of SNDX-275 and X-irradiation. SERs for BT-16 at SF_{0.1} were 1.61 (1 μM SNDX-275) and 1.75 (2 μM SNDX-275) and, at SF_{0.5}, were 1.72 (1 μM) and 1.89 (2 μM).

Discussion

Despite some advancements^{6,7,31} in the treatment of ATRT, long-term outcomes remain suboptimal. In addition, current multimodality therapy for this tumor has proven to be toxic and can be associated with late effects, most notably from intensive radiation dosing delivered to young children. Clearly, ATRT is a malignancy that requires evaluation of newer therapies to improve survival and minimize toxicity.

We have demonstrated in this study that HDI treatment of ATRT cell lines in vitro results in reduced cellular proliferation as measured by MTS and clonogenic assays. In addition, we have shown that a primary ATRT patient sample responds to HDI treatment in a similar manner when compared with established cell lines. Furthermore, we found that the HDI SNDX-275 induces apoptosis in BT-12 and BT-16 cell lines when administered at an IC₅₀ and results in increased p21^{Waf1/Cip1} tumor suppressor expression. These aspects of our study correlate to previous evaluations that examined the efficacy of HDAC inhibition on rhabdoid cell lines in vitro. In Furchert et al,²⁶ HDAC inhibition by SNDX-275 decreased proliferation of the BT-12 and BT-16 cell lines, but at higher micromolar concentrations than described in our study. In addition, 7.5 μM SNDX-275 was able to elicit an apoptotic response in BT-12 cells after 48 h of incubation. However, in our study, we observed an apoptotic

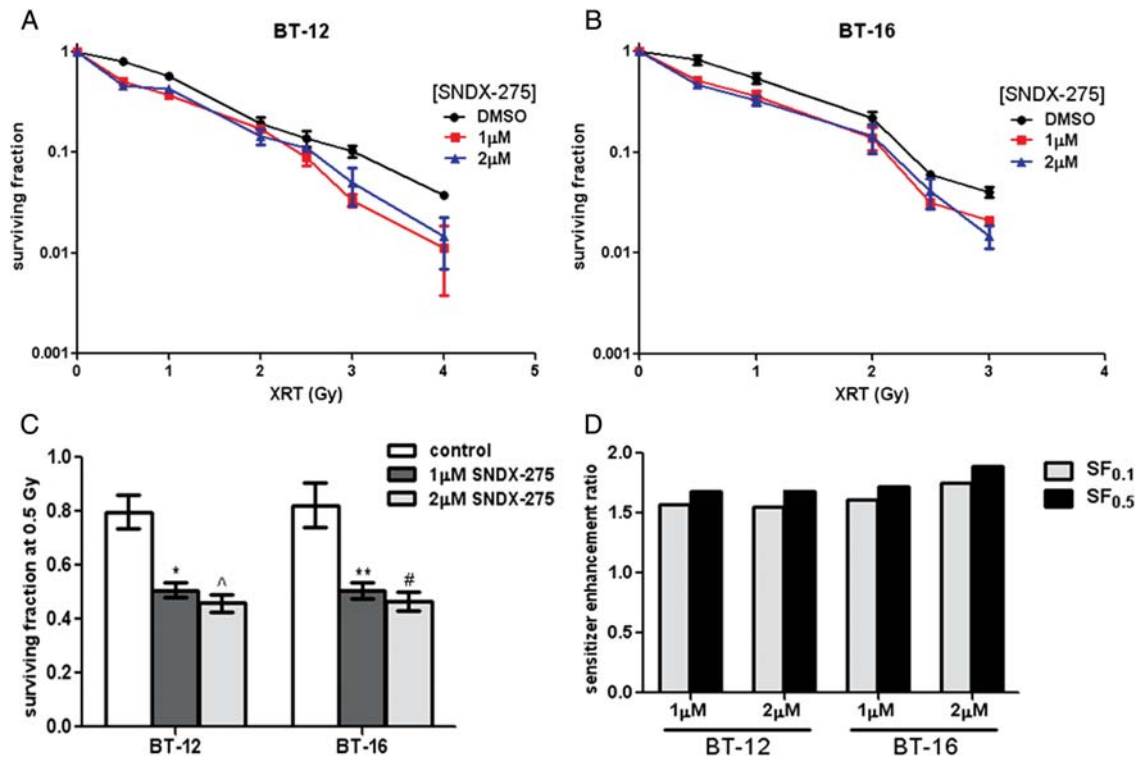


Fig. 5. SNDX-275 potentiates the effect of ionizing radiation on atypical teratoid/rhabdoid tumor (ATRT) cells. BT-12 (A) and BT-16 (B) cells were exposed to DMSO or SNDX-275 for 24 h and then exposed to varying doses of X-irradiation. Colony formation was determined 10–12 days later, and survival curves were generated. (C) Survival fractions after 0.5 Gy X-irradiation of BT-12 and BT-16 cells treated with DMSO or SNDX-275. * $P = .003$; ^ $P = .001$; ** $P = .01$; # $P = .005$ (P values calculated versus DMSO control for corresponding cell line). (D) Sensitizer enhancement ratios of BT-12 and BT-16 cells calculated at 10% (SF_{0.1}) or 50% (SF_{0.5}) cell survival. SF_{0.1} and SF_{0.5} radiation doses were determined using nonlinear regression analysis of survival curves (shown in Supplementary Fig. S4).

effect of SNDX-275 on BT-12 cells at a much lower concentration. Jaboin et al described the efficacy of SNDX-275 on the renal rhabdoid cell line G401.²⁴ In their study, 1 μM SNDX-275 treatment resulted in cell cycle arrest of G401 cells at 24 and 48 h after drug treatment. In addition, they found that transcription of the p21 tumor suppressor gene (*CDKN1A*) was induced by SNDX-275. The HDI romidepsin has also shown in vitro activity against non-CNS rhabdoid tumor cell lines G401 and STM91-01.²⁷ In that study, romidepsin was able to induce cell cycle arrest and restore *CDKN1C* tumor suppressor gene expression. Of interest, they also found that forced expression of *SMARCB1* in rhabdoid tumor cell lines was associated with increased histone H3 and H4 acetylation at the *CDKN1C* promoter. In vivo data has also demonstrated that HDAC inhibition by the HDI depsipeptide results in slower ATRT tumor growth and control in a xenograft model using the BT-40 cell line.²⁵

By evaluating differential gene expression altered by SNDX-275 treatment, we have shown that several key cellular processes are altered by HDI activity. To our knowledge, this is the first study to assess the genomic response to HDAC inhibition in rhabdoid tumor. Of note is the significant alteration of genes involved in cellular growth and proliferation, DNA replication, recombination, and repair and cell cycle. The alterations of

these biologic functions correlate well to our data demonstrating the antiproliferative effects of HDAC inhibition on BT-12 and BT-16 cells. Of interest, we specifically found the known tumor suppressor genes *CDKN2B* and *CDKN2D* to be upregulated in response to SNDX-275 treatment. Other key biologic processes in malignancy, such as cellular development, cellular movement, and inflammatory response, were also significantly altered by HDAC inhibition. Further investigation will be required to determine these processes' specific roles in the ATRT response to HDIs. In addition, evaluation of these pathways may prove to be valuable as biological markers of drug response in future experimentation because most current clinical studies focus on histone acetylation as the primary pharmacodynamic parameter.^{32–35}

It has previously been shown that cells with loss of *SMARCB1* are more sensitive to DNA damage,³⁶ and we have demonstrated that ATRT is certainly a radiosensitive tumor. Because the effect of radiation can be increased in the context of preexisting DNA damage, it is particularly intriguing that pretreatment with HDIs could enhance the radioresponsiveness of ATRT. This suggests that HDIs lead to DNA damage, a hypothesis that is supported by findings of increased γH2AX foci after HDI treatment of glioma and prostate carcinoma cell lines.²⁰ Our study has demonstrated that

SNDX-275 sensitizes ATRT cells to radiation at relatively low drug concentrations and radiation doses. This is presumptively attributable to enhanced, HDI-induced DNA damage, but further studies will be required to elucidate the mechanisms behind this phenomenon. We did, however, observe that 1 of the top 10 biologic networks differentially altered by HDI treatment of BT-12 and BT-16 cells was DNA replication, recombination, and repair. In the clinical setting, the ability of HDAC inhibition to potentiate the effect of radiation in ATRT may allow for the administration of lower radiation doses without sacrificing efficacy. The lower doses could, in turn, aid in decreasing long-term effects seen in young children who receive radiation to the CNS.

HDIs are currently being evaluated in multiple adult clinical trials, including 20 currently active or completed for SNDX-275 administered alone or in combination with other agents.³⁷ However, very few pediatric clinical studies with HDIs have been published to date. In a phase I study, depsipeptide was administered to children with recurrent or refractory solid tumors.³⁸ Although there were no objective responses, the HDI was being used as monotherapy, and the primary goal of the trial was to evaluate dosing. Of note, no patients with ATRT were included in that study. Certainly, further investigation into combination therapy will be needed to evaluate HDIs in the pediatric population because of the in vitro evidence that HDIs frequently function optimally when administered with other treatments. Although HDIs likely have limited use as monotherapy in highly malignant tumors, we believe that our in vitro studies warrant further investigation of the use of HDIs in the context of ATRT, particularly in combination with current therapeutic modalities.

Supplementary Material

Supplementary material is available at *Neuro-Oncology Journal* online (<http://neuro-oncology.oxfordjournals.org/>).

Acknowledgments

We thank Deb DeRyckere, Lori Gardner, Peter Harris, and Meg Macy for their technical advice and the University of Colorado Denver Microarray Core for their assistance with the microarray data.

Presented in part: American Society of Pediatric Hematology/Oncology annual meeting, Montreal, Quebec, Canada, April 7–10, 2010 (Poster 294), and Children's Oncology Group fall meeting, Dallas, Texas, September 21–24 2010.

Conflict of interest statement. None declared.

Funding

This work was supported by the National Institutes of Health Ruth L. Kirschstein National Research Service Award (T32CA082086 to J.K.), National Institute of Neurological Disorders and Stroke (K08NS59790 to R.V.), and Morgan Adams Foundation to N.F.

References

- Biggs PJ, Garen PD, Powers JM, Garvin AJ. Malignant rhabdoid tumor of the central nervous system. *Hum Pathol*. 1987;18(4):332–337.
- Rorke LB, Packer RJ, Biegel JA. Central nervous system atypical teratoid/rhabdoid tumors of infancy and childhood: definition of an entity. *J Neurosurg*. 1996;85(1):56–65.
- Bambakidis NC, Robinson S, Cohen M, Cohen AR. Atypical teratoid/rhabdoid tumors of the central nervous system: clinical, radiographic and pathologic features. *Pediatr Neurosurg*. 2002;37(2):64–70.
- Hilden JM, Meerbaum S, Burger P, et al. Central nervous system atypical teratoid/rhabdoid tumor: results of therapy in children enrolled in a registry. *J Clin Oncol*. 2004;22(14):2877–2884.
- Reddy AT. Atypical teratoid/rhabdoid tumors of the central nervous system. *J Neurooncol*. 2005;75(3):309–313.
- Gardner SL, Asgharzadeh S, Green A, Horn B, McCowage G, Finlay J. Intensive induction chemotherapy followed by high dose chemotherapy with autologous hematopoietic progenitor cell rescue in young children newly diagnosed with central nervous system atypical teratoid rhabdoid tumors. *Pediatr Blood Cancer*. 2008;51(2):235–240.
- Chi SN, Zimmerman MA, Yao X, et al. Intensive multimodality treatment for children with newly diagnosed CNS atypical teratoid rhabdoid tumor. *J Clin Oncol*. 2009;27(3):385–389.
- Biegel JA, Tan L, Zhang F, Wainwright L, Russo P, Rorke LB. Alterations of the hSNF5/INI1 gene in central nervous system atypical teratoid/rhabdoid tumors and renal and extrarenal rhabdoid tumors. *Clin Cancer Res*. 2002;8(11):3461–3467.
- Biegel JA, Zhou JY, Rorke LB, Stenstrom C, Wainwright LM, Fogelgren B. Germ-line and acquired mutations of INI1 in atypical teratoid and rhabdoid tumors. *Cancer Res*. 1999;59(1):74–79.
- Fujisawa H, Misaki K, Takabatake Y, Hasegawa M, Yamashita J. Cyclin D1 is overexpressed in atypical teratoid/rhabdoid tumor with hSNF5/INI1 gene inactivation. *J Neurooncol*. 2005;73(2):117–124.
- Botrugno OA, Santoro F, Minucci S. Histone deacetylase inhibitors as a new weapon in the arsenal of differentiation therapies of cancer. *Cancer Lett*. 2009;280(2):134–144.
- Duvic M, Talpur R, Ni X, et al. Phase 2 trial of oral vorinostat (suberoylanilide hydroxamic acid, SAHA) for refractory cutaneous T-cell lymphoma (CTCL). *Blood*. 2007;109(1):31–39.
- Garcia-Manero G, Yang H, Bueso-Ramos C, et al. Phase 1 study of the histone deacetylase inhibitor vorinostat (suberoylanilide hydroxamic acid [SAHA]) in patients with advanced leukemias and myelodysplastic syndromes. *Blood*. 2008;111(3):1060–1066.
- Glozak MA, Seto E. Histone deacetylases and cancer. *Oncogene*. 2007;26(37):5420–5432.

15. Lee MJ, Kim YS, Kummar S, Giaccone G, Trepel JB. Histone deacetylase inhibitors in cancer therapy. *Curr Opin Oncol*. 2008;20(6):639–649.
16. Xu WS, Parmigiani RB, Marks PA. Histone deacetylase inhibitors: molecular mechanisms of action. *Oncogene*. 2007;26(37):5541–5552.
17. Campas-Moya C. Romidepsin for the treatment of cutaneous T-cell lymphoma. *Drugs Today (Barc)*. 2009;45(11):787–795.
18. Mann BS, Johnson JR, Cohen MH, Justice R, Pazdur R. FDA approval summary: vorinostat for treatment of advanced primary cutaneous T-cell lymphoma. *Oncologist*. 2007;12(10):1247–1252.
19. Carey N, La Thangue NB. Histone deacetylase inhibitors: gathering pace. *Curr Opin Pharmacol*. 2006;6(4):369–375.
20. Camphausen K, Burgan W, Cerra M, et al. Enhanced radiation-induced cell killing and prolongation of gammaH2AX foci expression by the histone deacetylase inhibitor MS-275. *Cancer Res*. 2004;64(1):316–321.
21. Camphausen K, Cerna D, Scott T, et al. Enhancement of in vitro and in vivo tumor cell radiosensitivity by valproic acid. *Int J Cancer*. 2005;114(3):380–386.
22. Camphausen K, Tofilon PJ. Inhibition of histone deacetylation: a strategy for tumor radiosensitization. *J Clin Oncol*. 2007;25(26):4051–4056.
23. Jung M, Kozikowski A, Dritschilo A. Rational design and development of radiation-sensitizing histone deacetylase inhibitors. *Chem Biodivers*. 2005;2(11):1452–1461.
24. Jaboin J, Wild J, Hamidi H, et al. MS-27–275, an inhibitor of histone deacetylase, has marked in vitro and in vivo antitumor activity against pediatric solid tumors. *Cancer Res*. 2002;62(21):6108–6115.
25. Graham C, Tucker C, Creech J, et al. Evaluation of the antitumor efficacy, pharmacokinetics, and pharmacodynamics of the histone deacetylase inhibitor depsipeptide in childhood cancer models in vivo. *Clin Cancer Res*. 2006;12(1):223–234.
26. Furchert SE, Lanvers-Kaminsky C, Juergens H, Jung M, Loidl A, Fruhwald MC. Inhibitors of histone deacetylases as potential therapeutic tools for high-risk embryonal tumors of the nervous system of childhood. *Int J Cancer*. 2007;120(8):1787–1794.
27. Algar EM, Muscat A, Dagar V, et al. Imprinted CDKN1C is a tumor suppressor in rhabdoid tumor and activated by restoration of SMARCB1 and histone deacetylase inhibitors. *PLoS One*. 2009;4(2):e4482.
28. Vibhakhar R, Foltz G, Yoon JG, et al. Dickkopf-1 is an epigenetically silenced candidate tumor suppressor gene in medulloblastoma. *Neuro Oncol*. 2007;9(2):135–144.
29. El-Sheikh A, Fan R, Birks D, Donson A, Foreman NK, Vibhakhar R. Inhibition of Aurora Kinase A enhances chemosensitivity of medulloblastoma cell lines. *Pediatr Blood Cancer*. 2010;55(1):35–41.
30. Edgar R, Domrachev M, Lash AE. Gene Expression Omnibus: NCBI gene expression and hybridization array data repository. *Nucleic Acids Research*. 2002;30(1):207–210.
31. Tekautz TM, Fuller CE, Blaney S, et al. Atypical teratoid/rhabdoid tumors (ATRT): improved survival in children 3 years of age and older with radiation therapy and high-dose alkylator-based chemotherapy. *J Clin Oncol*. 2005;23(7):1491–1499.
32. Gojo I, Jiemjit A, Trepel JB, et al. Phase 1 and pharmacologic study of MS-275, a histone deacetylase inhibitor, in adults with refractory and relapsed acute leukemias. *Blood*. 2007;109(7):2781–2790.
33. Gore L, Rothenberg ML, O'Bryant CL, et al. A phase I and pharmacokinetic study of the oral histone deacetylase inhibitor, MS-275, in patients with refractory solid tumors and lymphomas. *Clin Cancer Res*. 2008;14(14):4517–4525.
34. Kummar S, Gutierrez M, Gardner ER, et al. Phase I trial of MS-275, a histone deacetylase inhibitor, administered weekly in refractory solid tumors and lymphoid malignancies. *Clin Cancer Res*. 2007;13(18 Pt 1):5411–5417.
35. Ryan QC, Headlee D, Acharya M, et al. Phase I and pharmacokinetic study of MS-275, a histone deacetylase inhibitor, in patients with advanced and refractory solid tumors or lymphoma. *J Clin Oncol*. 2005;23(17):3912–3922.
36. Klochendler-Yeivin A, Picarsky E, Yaniv M. Increased DNA damage sensitivity and apoptosis in cells lacking the Snf5/INI1 subunit of the SWI/SNF chromatin remodeling complex. *Mol Cell Biol*. 2006;26(7):2661–2674.
37. National Cancer Institute. Available at <http://www.cancer.gov/clinicaltrials>. Accessed August 30, 2011.
38. Fouladi M, Furman WL, Chin T, et al. Phase I study of depsipeptide in pediatric patients with refractory solid tumors: a Children's Oncology Group report. *J Clin Oncol*. 2006;24(22):3678–3685.